The effect of frictional contact properties on intermeshed steel connections

The effect of frictional contact properties on intermeshed steel connections

Matis, P.[1], Martin, T.[1], McGetrick, P.J.[1], Robinson, D.[1]
[1]School of Natural and Built Environment, David Keir Building, Queen's University Belfast, BT9 5AG, Northern Ireland
email: pmatis01@qub.ac.uk, t.martin@qub.ac.uk, p.mcgetrick@qub.ac.uk, des.robinson@qub.ac.uk

ABSTRACT: Modern built environment and infrastructure rely heavily on the use of steel structures. New manufacturing capabilities offer the potential to develop faster and more cost-effective connection methods for these structures, such as multi-storey steel buildings, potentially providing savings in weight, time and cost. To achieve these savings, improved construction efficiency and heightened material reuse, computer-controlled advanced manufacturing techniques in laser cutting enables the development of connections whose behaviour relies on the interlocking and friction between steel components. This paper presents the numerical modelling and experimental testing of a steel plate in direct tension; incorporating an intermeshed connection. A series of experimental tests were performed to capture the behaviour and failure modes of the steel plate connection under tension. The full load-displacement responses of the connection specimens were recorded and are presented and discussed here. A 2D finite element (FE) modelling programme was performed in parallel with the experimental study using the ABAQUS structural analysis software. The 2D FE model accounts for material and geometric non-linearity, large deformation and contact behaviour. Once the model was calibrated and validated against the experimental results, a parametric study was carried out to further investigate the influence of individual key parameters, focusing on the friction coefficient between the surfaces of the connections in contact and including variation of the plate thickness. This parametric study was performed to develop a comprehensive understanding of the behaviour of the intermeshed steel plate connections in tension.

KEY WORDS: ABAQUS; Advanced manufacturing techniques; Contact; Experimental testing; Finite element modelling; Friction coefficient; Intermeshed steel connection.

1 INTRODUCTION

For structural steel, the two main connection methods (i.e. bolting and welding) are based on century-old technologies. Both are expensive and time consuming while easy disassembly cannot always be facilitated for material reuse, particularly in the case of welding. Current steel fabrication practice favours the welding process, carried out in fabrication shops (as opposed to onsite) due to the high-quality control that can be achieved. This process is undertaken by highly experienced and certified welders. However, the subsequent transportation of the elements to the site limits the size of the assemblage that can be constructed in the shop. Moreover, further assembly on-site is then necessary which is challenging due to access and weather conditions [1]. Thus, the difficulty in guaranteeing a high-quality control for a successful weld is the requirement for extensive on-site testing. This adds time and direct costs to a construction project. The preferred connection method for on-site assembly is bolting since it is highly standardized [2]. Bolts are manufactured to specific standards and have a guaranteed performance. However, bolting on site is a slow manual process, as each bolt must be inserted and accurately tightened individually. In addition, deconstruction becomes difficult, particularly with welded connections, as welded steel must be cut at the structure’s end of life, with such steel being recycled.

Alternative steel connections have been developed during the last few decades. These connections provide functional solutions but have had limited application in practice. Among the most successful alternatives were the Kaiser connection, the Pin Fuse connection and the ConXtech connection [3]. However, these connections are complicated and expensive. Their design and their working mechanism is more complex and costly than equivalent bolted or welded connections. Many other patented connections were less successful since all of them continue to rely on conventional bolted or welded methods or need more expensive alternatives such as castings.

To address these drawbacks and to promote steel reuse and recycling, a new class of intermeshed steel connections using computer-controlled, advanced manufacturing techniques in laser cutting has been developed that rely on neither bolting nor welding [4,5]. This new method connects steel members that have precisely shaped ends in an interlocking approach. The connection is achieved by gravity-based placement of one end of a member relative to the end of another to create a robust intermeshed connection able to transfer force through common bearing surfaces. The connection can then be secured by manually inserting a small locking element. With that, three main advantages are achieved. First, members can be assembled faster than what is currently possible and at considerably reduced cost. Second, manual operations are reduced thus the final quality is significantly improved. Third, separating the connected parts at a future time for recycling or reuse is substantially easier, faster and cheaper. These advantages address priority actions outlined by the UK Roadmap for Energy Efficient Buildings [6] and are in addition to improved safety procedures and significantly less reliance on skilled workers. Due to its nature the new intermeshed steel connection does not require the addition of new components or materials such as bolts, welds or end plates. Due to precise nature of this connection method, work is ongoing on the accommodation of site erection tolerances according to BS EN 1090-2 [7], which is outside the scope of this paper.

This paper presents the numerical modelling and experimental testing of an intermeshed steel plate connection in direct tension; incorporating a parametric study on the frictional contact properties. A 2D finite element analysis (FEA) was performed in parallel with the experimental study using the ABAQUS structural analysis software. Once the 2D finite element (FE) model was calibrated and validated against the experimental results, a parametric study was carried out to further investigate the influence of individual key parameters such as the friction coefficient between the surfaces of the connections in contact and the variation of the plate thickness. The result of this parametric study was the development of a comprehensive understanding in the behaviour of the intermeshed steel plate connections under tension.

2 EXPERIMENTAL STUDY: SUMMARY

A series of tensile material tests and steel plate connection tests were carried out to investigate the structural behaviour of the new steel connection in tension. All tests were performed in the Heavy Structures laboratory at Queen's University Belfast. A series of material test samples were prepared from 6 mm thick S275JR steel plate. The results of these tests were used in Nonlinear Finite Element Analyses (NLFEA) of the novel steel plate connection. In parallel with material testing, the new connection geometry, composed of 6 mm S275JR steel plate, and cut using two alternative methods, was tested in tension up to ultimate failure.

Tensile 'dogbone' tests were performed to establish the basic material stress-strain response. This was subsequently utilised in the development of the numerical model. The tests were carried out in accordance with BS EN ISO 6892-1 [8]. The dimensions of the tensile samples are illustrated in Figure 1. These samples were tested by applying tensile loads under displacement control to samples taken from the 6 mm thick plate. Connection samples were also later fabricated from these plates. For each plate used in the testing programme, at least six representative samples were tested. These test samples were spray painted with a matt black and white speckle pattern. The speckle pattern was then identified and tracked by a digital image correlation (DIC) high resolution camera system (StrainMaster, LaVision, [9]).

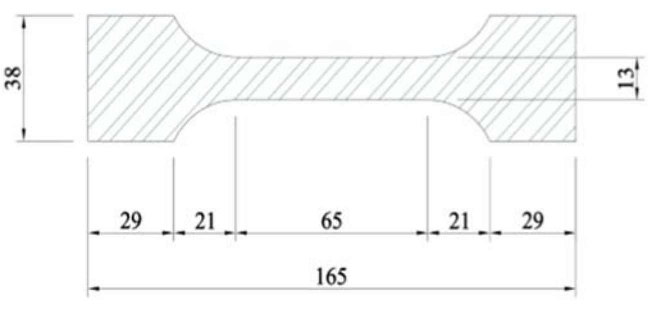

Figure 1. Dimensions of material tensile samples in mm.

All tensile tests (material and connections) were carried out using a RetroLine tC II universal testing machine (UTM) manufactured by Zwick/Roell, with a tensile capacity of 100 kN; the system was controlled via a computer running Zwick/Roell 'TestXpert II' software. The average material yield and ultimate strengths obtained from testing were 281 N/mm^2 and 371 N/mm^2 respectively.

The intermeshed steel plate connection was tested in direct tension to assess load carrying capacity and deformation. Full load displacement curves were recorded, including into the post-ultimate range. The geometry of the tested connection plate is shown in Figure 2. A total of 24 connections were tested from the 6 mm thick plate, which was cut using both waterjet and laser cutting methods. The tests were carried with the same RetroLine tC II universal testing machine (UTM) and the same DIC camera system used for material tensile testing.

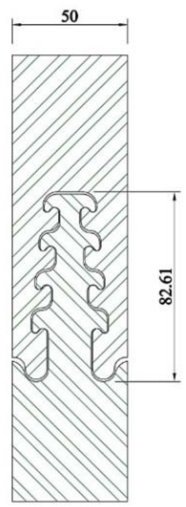

Figure 2. Plan view of steel plate connection geometry investigated (units in mm).

As mentioned earlier, connection test samples were spray painted with a black and white speckle pattern required for identification and tracking of displacements by the digital image correlation (DIC) camera system. Once this paint pattern had dried, test samples were placed within the wedge action grips of the tensile testing machine calibrated in accordance with ISO 7500-1 [10] and extension was applied at a vertical displacement rate of 1 mm/min.

The average load capacity of the connection samples tested was 43.7 kN, with yield occurring at 30.1 kN. For most samples, ultimate failure occurred due to fracture at the base of the lower 'male' section, as illustrated in Figure 5(a), although some outward splaying of the upper 'female' section also occurred. Although the geometry promotes interlocking between the male and female parts, the friction coefficient is also an important factor here due to both parts remaining in direct contact throughout testing until failure. All flange connection samples exhibited a similar failure mode except for three samples, where upper and lower sections slipped apart due to excessive in-plane and out-of-plane deformation resulting from localised material yielding before fracture occurred.

3 FINITE ELEMENT MODELLING

3.1 Introduction

A numerical modelling programme was implemented in parallel with experimental testing, using the non-linear finite element analysis software ABAQUS, Version 6.14 [11]. 2D plane stress nonlinear FE analyses were carried out which incorporated material and geometric nonlinearities, large deformations and contact conditions. Fracture of the material was not considered in the FE analyses. Both implicit static and explicit dynamic solvers were used to conduct numerical simulations. The finite element employed in the present study was CPS4R, a 4-node bilinear plane stress, quadrilateral shell element with reduced integration and hourglass control which has performed well in similar applications. A mesh convergence study was then carried out to establish a mesh size which would produce accurate results whilst remaining computationally efficient; the adopted mesh is shown in Figure 4.

3.2 FE modelling of flange connections

Geometric data and experimentally derived material properties were used in FE models to replicate the connection test behaviour. For the linear elastic response of the steel material of the connection the Young's modulus, E was taken as 210 GPa and the Poisson's ratio, v as equal to 0.3. To predict yielding in steel material, the von Mises yield criterion was employed. The material test data took the form of engineering stress and strain. ABAQUS requires that the material properties are specified in terms of true stress σ_{true} and logarithmic plastic strain $\varepsilon_{\ln}^{pl}$, which can be derived from the engineering stress-strain curves through Equations (1) and (2).

$$\sigma_{true} = \sigma_{eng}(1+\varepsilon_{eng}) \quad (1)$$

$$\varepsilon_{ln}^{pl} = \ln(1+\varepsilon_{eng}) - \frac{\sigma_{true}}{E} \quad (2)$$

where σ_{eng} and ε_{eng} are engineering stress and strain respectively and E is the modulus of elasticity. The continuous engineering stress-strain curve was initially approximated with a multilinear curve which was subsequently converted into the required $\sigma_{true} - \varepsilon_{ln}^{pl}$ format, as shown in Figure 3.

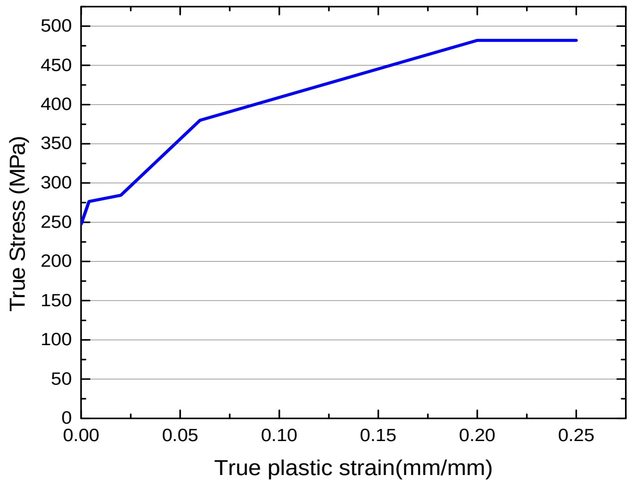

Figure 3. Multi-linear Plastic true stress-strain curve implemented in ABAQUS.

3.2.1 Contact and frictional properties

A surface-to-surface contact interaction was adopted for the numerical model. In this contact interaction, master-and-slave surfaces were defined and the surface with the coarser mesh was chosen as the master surface. The tangential behaviour was defined as a 'Penalty' friction formulation and the 'Coulomb' friction model was used with a friction coefficient of μ = 0.3 for the two contact surfaces. Early parametric studies performed by the authors showed that changing the Coulomb friction coefficient, μ, for tangential contact between the two surfaces of the intermeshed steel connection did not significantly affect its tensile behaviour. The normal contact behaviour was defined as a 'Hard' contact pressure overclosure relationship.

With respect to the boundary conditions, the lower edge of the flange connection was fixed, and the upper end was pulled vertically upwards during the analysis using displacement control until failure occurred. A series of FE meshes were simulated to assess the sensitivity of results to different FE mesh sizes. The result of this sensitivity study suggested that the appropriate mesh size should be 3.5 mm for the flange connection elements of the outside edges, as shown in Figure 4.

3.2.2 Numerical simulation solver

Both implicit static and explicit dynamic solvers were employed for the numerical simulations. An implicit static solver is commonly used in structural analyses. However, significant efforts are required to make the procedure convergent when contact conditions are simulated in the model. The explicit dynamic solver can overcome this problem. Although the explicit dynamic solver cannot provide the static response, the dynamic effect could be ignored if the kinetic energy of the deformed structure is only a fraction (typically 5% to 10%) of its internal energy throughout most of the structural response. Thus, a quasi-static simulation was also used in these analyses. In the present case, since large computational resources were required by the explicit dynamic solver, implicit static analyses were chosen.

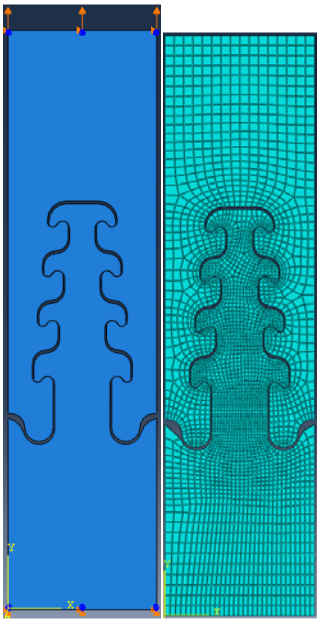

Figure 4. Typical FE model of the flange connection and its boundary conditions adopted for numerical simulations in ABAQUS.

In ductile crystalline materials such as steel, fracture initiation can be triggered by plasticity. Ductile fracture will occur after the material undergoes extensive necking and plastic deformation in the necked region (Yang et al., [12]). The ductile criterion in ABAQUS is a phenomenological model for predicting the onset of damage due to nucleation, growth and coalescence of voids. This model can simulate the fracture of the connection material which was observed during experimental investigations and will be used by the authors in future studies. However, in the current study, material fracture was not included in the FE model.

3.3 *Comparison between FE models and test results*

As discussed earlier for the experimental tests, in most cases, ultimate failure occurred due to fracture at the base of the lower (male) section of the flange connection, as illustrated in Figure 5. In this connection simulation, both the implicit static and explicit dynamic solvers have been used to simulate the test procedure. In order to obtain the full load-displacement curve of the flange plate connection, a displacement control method is employed for the numerical simulations in ABAQUS. This method is usually applied when the post-peak behaviour needs to be captured, especially from necking until ultimate failure. Predicted connection behaviour obtained from FEA which relates to failure modes are also shown in Figure 5, alongside an experimental test specimen. Each solver predicts both the failure mode and load-displacement curve well.

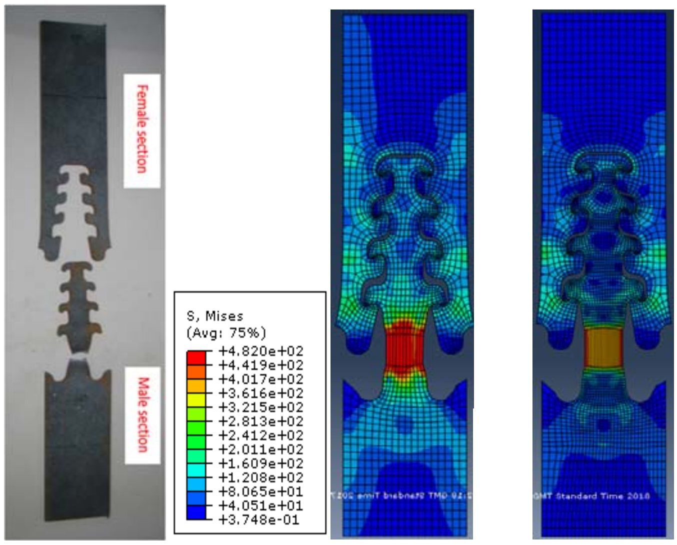

(a) Experiment (b) Implicit Static solver (c) Explicit dynamic solver

Figure 5. Failure modes of the FE simulation and experiment of the flange connection in direct tension. (Von Mises Stress Contours in MPa).

Overall, the 2D FE model has been found to be capable of replicating the experimentally observed tensile response of the flange connection. As shown in Figure 6, the predicted load-displacement curves closely agree with the experimental curve in both the elastic and plastic regions until the ultimate strength is reached i.e. as the behaviour transitions from strain hardening to softening. The explicit dynamic solver gives almost the same curve as the implicit static solver, although the latter is more numerically stable than the former. The initial stiffness and peak load of the modelled flange connection are generally well predicted. However, the post-ultimate response of the tested flange connection is not captured well by the 2D FE model.

This discrepancy in the post-ultimate behaviour, i.e. during strain softening, was due to the two-dimensional plane stress nature of the FE analysis performed and its inherent limitations. This 2D FE analysis can model strain softening behaviour, but cannot model any stress variation through the thickness of the plate – this variation is influenced by necking and contributed to the observed failure at a higher displacement in the experimental test (Figure 6). A 3D FE model can address this variation at a higher computational cost. However, the 2D plane stress FE model developed has a very good level of accuracy in general and offers advantages in terms of computational time and memory usage versus a detailed 3D FE model.

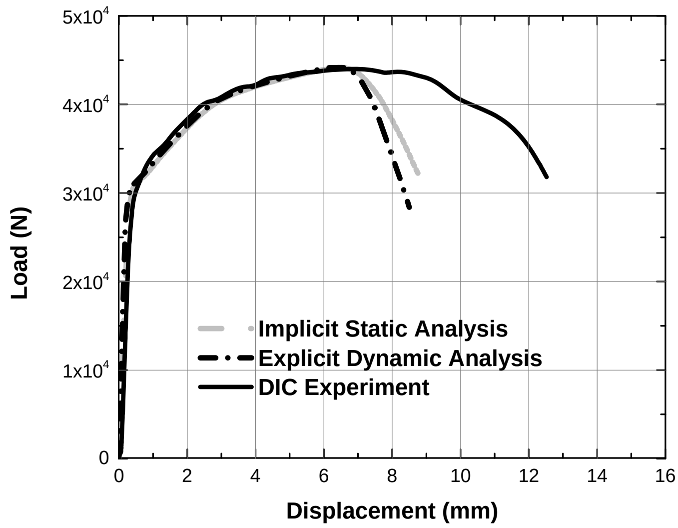

Figure 6. Comparison of the 2D FE simulations to the experimental data of the flange connection.

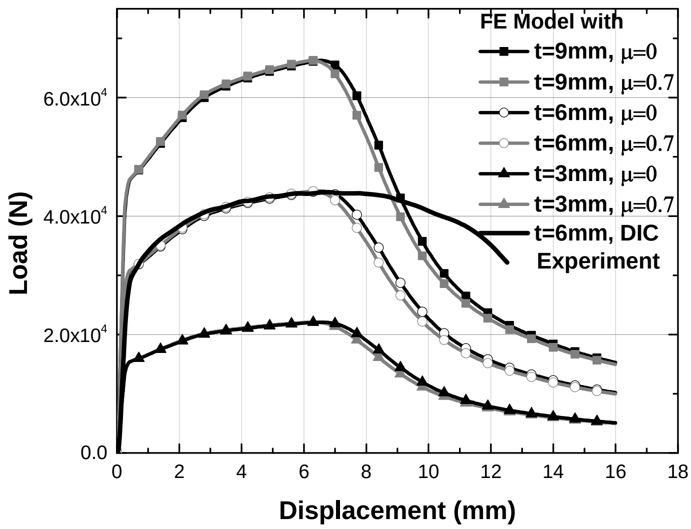

Figure 7. Effect of plate thickness, *t*, for two distinct values of friction coefficient on the intermeshed connection.

A PC with 64-bit System and Intel Core i7-6700 CPU at 3.4 GHz, 4 core with 8 logical processors was used for the numerical simulations. The average simulation time with the explicit dynamic solver was 2.5 hrs approximately while the implicit static solver took much less time, at approximately 15 minutes only.

4 PARAMETRIC STUDY

In this section, the 2D FE model described previously was used to investigate the influence of friction coefficient between the surfaces of the connection in contact, on the load-displacement behaviour of this connection under tension. In addition, another parameter governing the intermeshed connection, namely, plate thickness, is also varied.

The implicit static solver was used to conduct the parametric study for the intermeshed steel plate connection, since it is more efficient computationally and is commonly used for this type of analyses. As shown in Figure 7, the effect of plate thickness, t was studied by using three values of t, i.e. t = 3 mm, t = 6 mm and t = 9 mm. From this figure it can be observed that increasing the plate thickness from 3 mm to 9 mm increases the load-carrying capacity of the intermeshed steel plate connection in a proportional way. For this parameter, in each case, two distinct values of friction coefficient were considered, i.e. μ = 0 (slip condition) and μ = 0.7 (practically a 'stick' condition). These two extreme values of friction coefficient were used in order determine what is the largest possible range of effects that frictional contact can have on the behaviour of the intermeshed steel plate connection.

The variation in the intermeshed steel connection response due to the change in the friction coefficient can be observed. From Figure 7, comparisons between the two distinct values of friction coefficient can be made for each differing plate thickness of the intermeshed steel plate connection. It is evident that friction effects influence the connection behaviour in the elastic and post-peak range. However, this influence on the connection response is rather limited according to the two-dimensional plane stress FE model results. Therefore, to study these differences in more detail, Figure 8 presents the load difference (between the slip and stick condition) against displacement for each plate thickness.

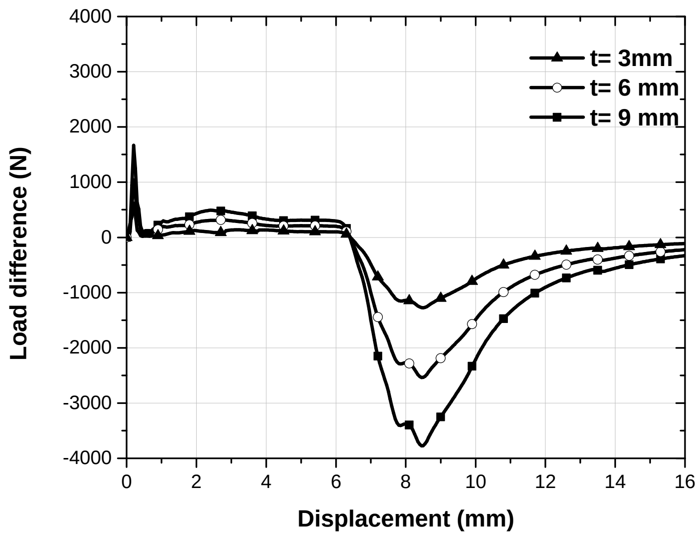

Figure 8. Load difference between μ = 0 and 0.7 against displacement for varying plate thickness.

Considering the post-peak range of the connection response in Figures 7 and 8, i.e. at displacements greater than approximately 7 mm, it can be ascertained that a friction coefficient equal to 0.7 resulted in connection behaviour with lower capacity and less ductility, compared to corresponding results for the friction coefficient equal to zero. Other friction coefficients (results not shown here) were found to produce behaviour fitting between these two extremes. Therefore, a constant friction coefficient of 0.3 was considered as ideal for the simulation of contact between the surfaces of the steel connection in the experiment. This is also in agreement with the corresponding slip factor (friction coefficient) for Class C of friction surfaces for slip-resistant bolted connections described in EN 1993-1-8 [13] and as allowed by the American Institute of Steel Construction (AISC) [14] and the Research Council on Structural Connections (RCSC) [15].

The effect of friction coefficient, although limited, is proportional to the plate thickness, as illustrated in Figure 8. Finally, Figure 9 also highlights this, showing that the load changes as percentages (between the two extreme values of friction coefficient, with respect to μ = 0.7) against displacement for each plate thickness follow the same relative trends, which is as expected.

It can be observed that in the linear range, for varying plate thickness the maximum load change is approximately 6% (between the two extreme values of friction coefficient) whereas, in the post-peak region is slightly higher to 7.5%.

Further parametric investigation using a more detailed 3D FE is expected to confirm the observations for the 2D model; preliminary investigations show that the influence of the friction coefficient is higher in a 3D FE model due to the consideration of stress distribution through the thickness of the plate and is therefore more appropriate for modelling post-peak i.e. strain softening behaviour where required.

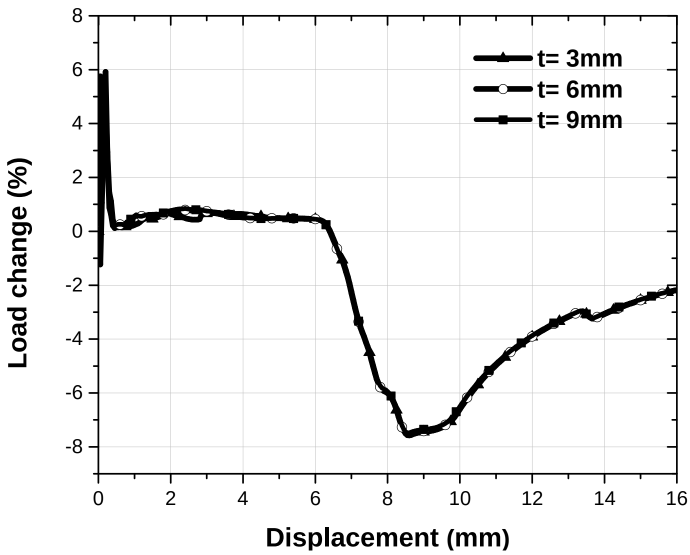

Figure 9. Load change (%) between μ = 0 and 0.7 against displacement for varying plate thickness.

5 CONCLUSIONS

This paper presents the numerical modelling and experimental testing of a steel plate in direct tension; incorporating an intermeshed connection. 2D finite element analysis was performed in parallel with the experimental study using ABAQUS structural software. In this research the authors used both implicit static and explicit dynamic solvers to conduct 2D numerical simulations. It has been shown that the 2D finite element models correlated well with test results, excluding the post-ultimate behaviour. Once the 2D FE models were calibrated and validated against the experimental results, a parametric study was carried out to further investigate the influence of individual key parameters with the use of implicit static solver. The parameters were the friction coefficient between the surfaces of the connections in contact and the variation of the plate thickness. The result of this parametric study was the development of a more comprehensive understanding in the behaviour of the intermeshed steel plate connections under tension.

In all cases, contact interaction was crucial for modelling the intermeshed flange connection performance. Several conclusions can be drawn based on the results of FE analyses and the parametric study:

i. A simple 2D plane stress FE model incorporating contact and non-linear geometric and material properties can be used to accurately model the intermeshed flange plate connection behaviour in direct tension using ABAQUS/Standard and ABAQUS/Explicit software.

ii. The flange connection model has been successfully created and validated against experimental test data and was used for a parametric study.

iii. The proposed finite element models may be used as benchmarks to verify the accuracy of similar flange connection geometries in tension incorporating contact, geometric and material non-linearity.

iv. Almost the same predictions have been observed for both implicit static and explicit dynamic solvers. However, the implicit static solver is recommended for these analyses due to higher efficiency in terms of computational time.

v. Contact interaction between the two parts has been shown to have a significant influence on the tensile behaviour of the intermeshed flange connection.

vi. Overall, the influence of friction coefficient on the connection response is relatively insignificant. Its limited effect however is dependent on the plate thickness.

vii. Following this analysis, a friction coefficient of value of μ = 0.3 is adopted which is also in agreement with the Eurocode 3 [10] design recommendations for slip-resistant bolted connections of class C friction surfaces, and Class A for AISC [11].

viii. The proposed 2D FE model, however, could not accurately predict the post-ultimate behaviour of the intermeshed flange plate connection. Detailed 3D FE analyses are required in these cases, but with the disadvantage of using comparatively significant computational resources.

ACKNOWLEDGMENTS

The research presented in this paper is part of a collaboration and partnership between Queen's University Belfast (QUB), University College Dublin (UCD) and the University of Minnesota (UMN). The authors wish to express their gratitude for the funding received from the US-Ireland Research and Development Partnership Programme, supported by DfE and Invest NI.

REFERENCES

[1] Bansal, R. K. A textbook of Strength of Materials, 3rd Edition, Laxmi Publications, 902-912, 1996.
[2] Mao, C., Ricles, J., Lu, L.W. and Fisher, J. Effect of local details on ductility of welded moment connections, Journal of Structural Engineering. 127:1036-1044, 2001
[3] Cordova P.P. and Hamburger, R.O. Steel connections: Proprietary or public domain, Modern Steel Construction 51(10):24-31, 2011.
[4] Al Sabah, A., Laefer, D. (2017a). Structural Member. GB Patent Application No 1718744.4. Filed November 13 2017.
[5] Al Sabah, A., Laefer, D. (2017b). Structural Member. GB Patent Application No 1718746.9. Filed November 13 2017.
[6] UK Roadmap for Energy Efficient Buildings. National Platform for the Built Environment, UK, 2012.
[7] BS EN 1090-2:2008+A1. Execution of steel structures and aluminium structures - Part 2: Technical requirements for steel structures, London: BSI Group, 2011.
[8] BS EN ISO 6892-1. Metallic materials — Tensile testing Part 1: Method of test at room temperature, London: BSI Group, 2016
[9] LaVision. StrainMaster Systems. 2017. [ONLINE] Available at: http://www.lavision.de/en/products/strainmaster/systems/index.php. [Accessed 14 May 2018].
[10] ISO 7500-1. Metallic materials. Verification of static uniaxial testing machines. Tension/compression testing machines. Verification and calibration of the force-measuring system, London: BSI Group, 2004.
[11] Dassault Systems Simulia. ABAQUS Analysis User's Manual, Version 6.14, 2014.
[12] Yang, B., Tan, K. H. Numerical analyses of steel beam-column joints subjected to catenary action, Journal of Constructional Steel Research 70:1-11, 2012.
[13] EN 1993-1-8. Eurocode 3-design of steel structures-Part 1-8: design of joints. Brussels: CEN, European Committee for standardization, 2005.
[14] AISC, Specifications for Structural Steel Buildings, AISC, Chicago, IL, 2010.
[15] AISC, Specifications for Structural Joints Using High Strength Bolts, 60601 Research Council of Structural Connections (RCSC), Chicago, Illinois, 2014.